JVI Journals.ASM.org

Bst2/Tetherin Is Induced in Neurons by Type I Interferon and Viral Infection but Is Dispensable for Protection against Neurotropic Viral Challenge

Alicia M. Holmgren,[a,b] Katelyn D. Miller,[b,c] Sarah E. Cavanaugh,[a,b] Glenn F. Rall[b]

Department of Microbiology and Immunology, Drexel University College of Medicine, Philadelphia, Pennsylvania, USA[a]; Program in Blood Cell Development and Function, Fox Chase Cancer Center, Philadelphia, Pennsylvania, USA[b]; Program in Cell and Molecular Biology, Perelman School of Medicine, University of Pennsylvania, Philadelphia, Pennsylvania, USA[c]

ABSTRACT

In permissive mouse central nervous system (CNS) neurons, measles virus (MV) spreads in the absence of hallmark viral budding or neuronal death, with transmission occurring efficiently and exclusively via the synapse. MV infection also initiates a robust type I interferon (IFN) response, resulting in the synthesis of a large number of genes, including bone marrow stromal antigen 2 (Bst2)/tetherin/CD317. Bst2 restricts the release of some enveloped viruses, but to date, its role in viral infection of neurons has not been assessed. Consequently, we investigated how Bst2 was induced and what role it played in MV neuronal infection. The magnitude of induction of neuronal Bst2 RNA and protein following IFN exposure and viral infection was notably higher than in similarly treated mouse embryo fibroblasts (MEFs). Bst2 synthesis was both IFN and Stat1 dependent. Although Bst2 prevented MV release from nonneuronal cells, its deletion had no effect on viral pathogenesis in MV-challenged mice. Our findings underscore how cell-type-specific differences impact viral infection and pathogenesis.

IMPORTANCE

Viral infections of the central nervous system can lead to debilitating disease and death. Moreover, it is becoming increasingly clear that nonrenewable cells, including most central nervous system neurons, combat neurotropic viral infections in fundamentally different ways than other rapidly dividing and renewable cell populations. Here we identify type I interferon signaling as a key inducer of a known antiviral protein (Bst2) in neurons. Unexpectedly, the gene is dispensable for clearance of neurotropic viral infection despite its well-defined contribution to limiting the spread of enveloped viruses in proliferating cells. A deeper appreciation of the importance of cell type heterogeneity in antiviral immunity will aid in the identification of unique therapeutic targets for life-threatening viral infections.

Many of the foundational principles in immunology have resulted from basic observations of virus-cell interactions, including the induction and antiviral function of both type I and type II interferons (IFNs) (reviewed in references 1, 2, and 3). Viral infection of a cell typically results in cellular production and secretion of type I IFNs, which can then bind to cell surface receptors in a paracrine and autocrine fashion, leading to synthesis of interferon-stimulated genes (ISGs). These ISGs, in turn, aid in clearing the viral infection by directly cleaving viral nucleic acids, triggering cellular apoptosis, inducing autophagy, upregulating major histocompatibility complex (MHC) class I expression to aid in $CD8^+$ T cell-mediated cytotoxicity, and preventing viral egress. Moreover, the induction of type I IFN contributes to the recruitment of adaptive immune effectors to infected sites, which further promotes viral clearance.

One ISG that is highly induced following infection by many viruses, and in response to both type I and II IFN signaling, is the gene for bone marrow stromal antigen 2 (Bst2; also known as HM1.24, tetherin, and CD317) (4). Bst2 was first discovered as a marker expressed on terminally differentiated B cells and in certain human hematopoietic malignancies (5). The discovery that Bst2 could directly prevent human immunodeficiency virus type 1 (HIV-1) virion release by tethering virus particles to an infected host cell ignited interest in this novel antiviral protein. The subsequent finding that the HIV-1 vpu protein directly antagonizes Bst2 underscored that viruses have evolved to modulate the antiviral role of this cellular protein (6–10). It has been shown that Bst2 can restrict budding of a variety of enveloped viruses, including Ebola virus, vesicular stomatitis virus (VSV), and herpes simplex virus 2 (HSV-2) (11–13).

Bst2 is a transmembrane protein thought to directly tether the viral membrane to the host cell membrane (reviewed in references 14, 15, and 16). Bst2 has also been shown to activate the NF-κB pathway, presumably further amplifying cellular stress signals (17). While the functional roles of Bst2 in uninfected cells are just emerging, it is clear that many viruses encode proteins that subvert Bst2's antiviral activities, often by altering clathrin-mediated endocytic pathways (18–20). To date, studies aimed at understanding Bst2's role in preventing viral infection have been limited

Received 8 July 2015 **Accepted** 17 August 2015

Accepted manuscript posted online 26 August 2015

Citation Holmgren AM, Miller KD, Cavanaugh SE, Rall GF. 2015. Bst2/tetherin is induced in neurons by type I interferon and viral infection but is dispensable for protection against neurotropic viral challenge. J Virol 89:11011–11018. doi:10.1128/JVI.01745-15.

Editor: D. S. Lyles

Address correspondence to Glenn F. Rall, glenn.rall@fccc.edu.

A.M.H. and K.D.M. contributed equally to this article.

to immune cells and rapidly dividing cell types such as fibroblasts (21). Although Bst2 has been shown to be induced in primary neurons following virus infection, whether it modulates the viral life cycle in these cells has not been explored (22, 23).

One of our laboratory's primary interests is to understand measles virus (MV) infection and spread within central nervous system (CNS) neurons. To study this, we use transgenic mice that express CD46, the first identified human MV receptor, under the control of the neuron-specific enolase promoter (NSE-CD46$^+$ mice) (24–26). Because mice are not normally permissive to MV infection, we can use this model to restrict viral replication to CNS neurons. MV spread within primary neurons that are obtained from these mice occurs through synaptic connections in the absence of extracellular viral release, distinct from the productive and lytic infection it causes in nonneuronal cells (23, 27, 28). Functional clearance of MV from the CNS of NSE-CD46$^+$ mice is noncytolytic and dependent on both T cells and gamma interferon (IFN-γ) (29, 30). Interestingly, neurons differ fundamentally in the basal levels of key signaling molecules that are required for ISG induction compared to mouse embryonic fibroblasts (MEFs) (31). During the course of previous studies, we identified numerous genes that were synthesized in primary hippocampal neurons and MEFs following IFN-γ treatment. From this list, Bst2 was among the top 5 induced genes (23). In this study, we investigated the induction and contribution of Bst2 in MV infection of CNS neurons both *in vivo* and *ex vivo*.

Using knockout mice and primary neuronal cell cultures, we showed that induction of Bst2 is dependent on Stat1 signaling induced by type I IFN and that Bst2 expression can restrict MV cellular egress in a rapidly dividing, nonneuronal cell type. Moreover, Bst2 is induced by IFN in neurons to a much greater extent than that observed in MEFs. Given this induction, we were surprised to find that the absence of Bst2 had no apparent effect on neuronal viral pathogenesis following infection of NSE-CD46$^+$ mice. Our data support a growing body of literature showing that neurons combat and control viral infections in fundamentally different ways than rapidly dividing cell types.

MATERIALS AND METHODS

Ethics statement. This study was carried out in accordance with the recommendations in the *Guide for the Care and Use of Laboratory Animals* of the National Research Council (32). The protocol was reviewed and approved by the Fox Chase Cancer Center Institutional Animal Care and Use Committee (Office of Laboratory Animal Welfare assurance number A3285-01).

Cell culture, interferon treatment, and virus infections. Primary hippocampal neurons were obtained from day 14 to 16 mouse embryos and cultured in Neurobasal medium (Gibco) supplemented with L-glutamine in the absence of an astrocyte feeder layer, as described previously (26–28). Neurons were plated on 15-mm glass coverslips or in 12-well plates coated with poly-L-lysine (Sigma-Aldrich) at a density of 2×10^5 cells/well, unless otherwise noted. Neuron cultures were frequently quality controlled and were routinely >95% Map2 positive. Neurons were plated and incubated for 5 days prior to IFN treatment or infection to allow for full differentiation. Primary mouse embryonic fibroblasts (MEFs) were isolated from the same embryos and maintained in complete Dulbecco modified Eagle medium (DMEM; supplemented with 10% fetal calf serum, 2 mM L-glutamine, 100 U/ml of penicillin, and 100 ng/ml of streptomycin). All cells were maintained at 37°C and 5% CO_2 in a humidified incubator.

For cells treated with IFNs, recombinant murine IFN-β or IFN-γ (Millipore) was diluted in B27-free Neurobasal medium, added to the cultures (100 U/ml final), and incubated for the desired times prior to collection.

MV-Edmonston (vaccine strain) was purchased from American Type Culture Collection (ATCC) and passaged and subjected to titer determination in Vero cells (monkey kidney fibroblasts). Passage 2 or 3 of the MV stock was used for all infections. Lymphocytic choriomeningitis virus (LCMV) Armstrong (LCMV-Arm; ATCC) was passaged and plaque purified in BHK-21 cells (baby hamster kidney fibroblasts), and titers were determined on Vero fibroblasts. All infections of primary cultures were carried out at a multiplicity of infection (MOI) of 1. Briefly, conditioned medium was removed and cells were inoculated with 500 μl of virus diluted in unconditioned Neurobasal medium or DMEM for 1 h at 37°C. After infection, cells were gently washed and conditioned medium was replaced until the desired time of harvest. 293T-Rex cells (Invitrogen) were modified to inducibly express Bst2 (293T-Bst2 cells) upon tetracycline exposure (1 μg/ml) and were a gift from Ju-Tao Guo (Drexel University). These cells were maintained as described in the original report (12). To induce Bst2 expression, cells were treated with tetracycline for 24 h and were then infected with MV at an MOI of 1.0 for 1 h. Virus was then removed and replaced with fresh medium, with or without tetracycline.

Western blot analyses. Whole-cell lysates for Western blot analysis were collected by scraping cells in 1× protein solubilization buffer (containing SDS and EDTA) and stored at −80°C until analysis. Protein was run into a 10% bis-Tris gel (Life Technologies) in morpholineethanesulfonic acid (MES) running buffer (Life Technologies) and transferred to an Immobilon membrane (Millipore). Membranes were blocked with Odyssey blocking buffer (Odyssey) and immunoblotted for glyceraldehyde-3-phosphate dehydrogenase (GAPDH; Millipore AB2302; 1:10,000) and Bst2 (Sigma PRS4661; 1:1,000). Secondary antibodies were obtained from LI-COR (IRDye 680RD donkey anti-chicken IgG [H+L]; IRDye 800CW donkey anti-rabbit IgG [H+L]). Images were captured with a LI-COR Odyssey classic infrared imager.

Reverse transcriptase quantitative real-time PCR (RT-qPCR). RNA was purified from whole-cell lysates using the RNeasy minikit (Qiagen). RNA was quantified using a NanoDrop spectrophotometer. RNA was reverse-transcribed using a high-capacity cDNA reverse transcription kit (Applied Biosystems) with random hexamer priming. Gene-specific primers were used in combination with probes designed using the Universal Probe Library algorithm (Roche) and Universal Master mix (Roche); all reactions were run on a Mastercycler Realplex2 system (Eppendorf). Cycling conditions were 50°C for 2 min and 95°C fir 10 min, followed by 40 (2-step) cycles (95°C for 15 s and 60°C for 60 s). Relative quantification to the control (cyclophilin B) was done using the comparative threshold cycle $\Delta\Delta CT$ method. Individual sample PCRs were performed in triplicate. The following gene specific primers (Integrated DNA Technologies) were used: Cyclophilin B Forward (5′-TTCTTCATAACC ACAGTCAAGACC-3′), Cyclophilin B Reverse (5′-ACCTTCCGTACCA CATCCAT-3′; UPL 20), Bst2 Forward (5′-GAAGTCACGAAGCTGAAC CA-3′), Bst2 Reverse (5′-CCTGCACTGTGCTAGAAGTCTC-3′; UPL 78); MV nucleoprotein Forward (5′-GGAAACTGCACCCTACATGG-3′), and MV nucleoprotein Reverse (5′-GGGTATGATCCTGCACTGAA CT-3′; UPL 80).

Mice and *in vivo infections*. Homozygous NSE-CD46$^+$ transgenic mice (line 18; H-2^b) (26) were maintained in the closed breeding colony of the Fox Chase Cancer Center. Homozygous NSE-CD46$^+$ and haplotype-matched homozygous immune knockout (KO) mice were intercrossed for three or more generations to obtain NSE-CD46$^+$ mice on the desired KO background. NSE-CD46$^+$/IFN-γ knockout and NSE-CD46$^+$/Stat1 knockout mice have been used in our lab previously (23, 30). IFNAR1-deficient mice on a 129S2/SvPas background were obtained from Luis Sigal (Fox Chase Cancer Center, Philadelphia, PA). Bst2 KO mice were obtained from Marco Colonna, Washington University, St. Louis, MO. Rag2 KO mice were obtained from Michael Oldstone, Scripps Research Institute, La Jolla, CA. The genotypes of mice used in these experiments were confirmed by PCR analysis of tail biopsy specimen DNA or fluores-

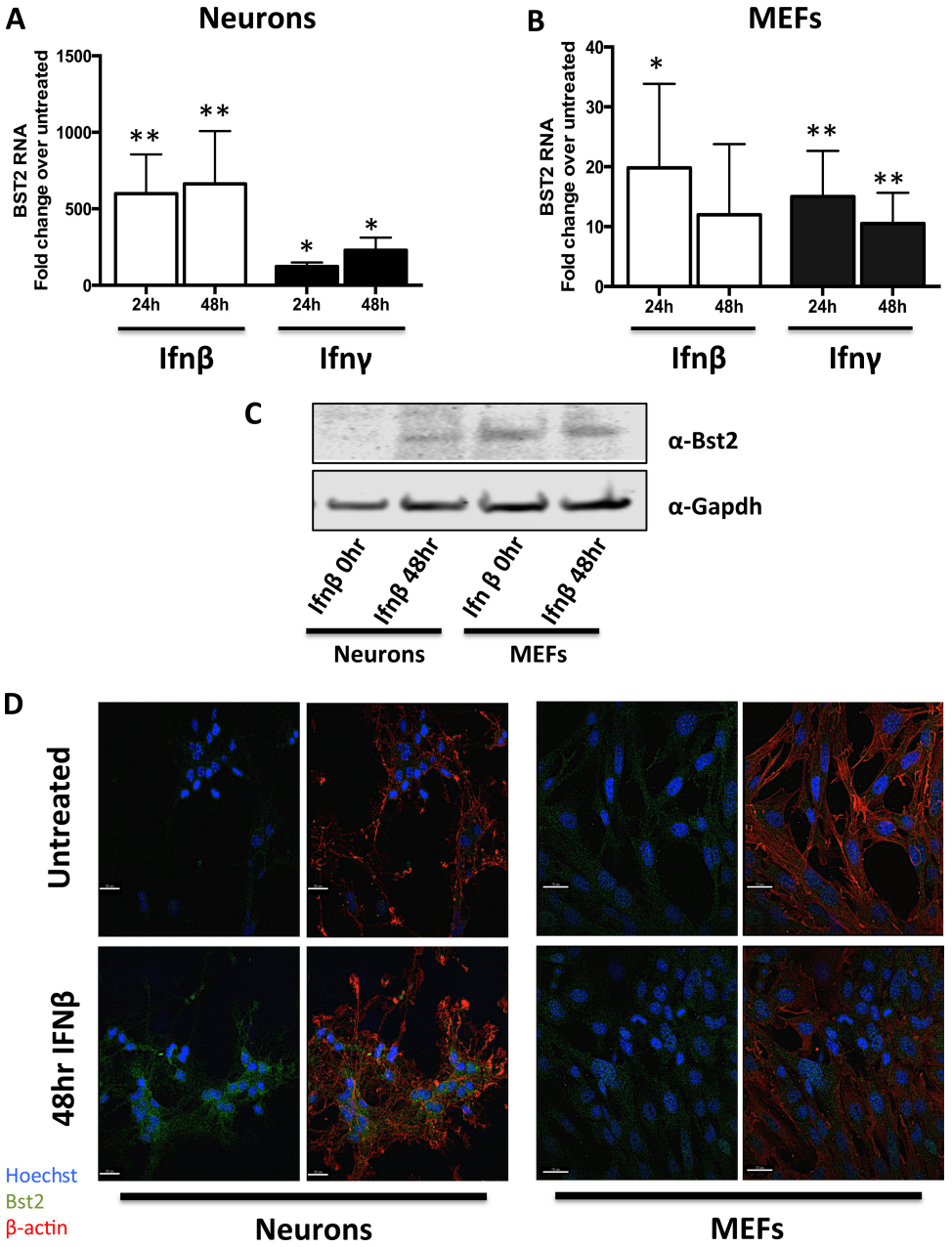

FIG 1 Bst2 RNA and protein are induced in both primary neurons and MEFs in response to interferon, but to a higher extent in neurons. Primary neurons spiked with mouse recombinant type I interferon (IFN-β) or type II interferon (IFN-γ), at a concentration of 100 U/ml, were assayed for changes in Bst2 RNA by RT-qPCR. Data are represented as fold change compared to value for untreated cells using the ΔΔ*CT* method. $n = 5$ per group. Results for the unpaired *t* test with equal-standard-deviation samples compared to the 0-h value for the same cell type are shown. **, $P < 0.005$; *, $P < 0.05$. Results of at least 3 independent experiments are presented. Error bars represent the standard deviations among groups. (A) Bst2 RNA abundance in primary neurons. (B) Bst2 RNA abundance in primary mouse embryo fibroblasts. (C) Western blot for Bst2 and GAPDH protein from primary neurons and MEFs following IFN exposure at a dose of 100 U/ml. The image was captured using LI-COR Odyssey. (D) Coverslips of primary neurons and MEFs that were spiked with 100 U/ml of IFN for 48 h or left untreated were stained for Bst2 (green), Hoechst (blue), and β-actin (red). Each sample set is shown as Bst2 and Hoechst staining (left) or as a merged image of Bst2, Hoechst, and β-actin (right). Primary neurons without (top) or with (bottom) IFN treatment (left side) and primary MEFs without (top) or with (bottom) IFN treatment (right side) are shown.

cence-activated cell sorter (FACS) analysis of blood collected from the orbital sinus.

Isoflurane-anesthetized mice were infected with MV-Edmonston via intracranial inoculation of 1×10^4 PFU in a volume of 30 μl, delivered along the midline using a 27-gauge needle. Mice were monitored daily postinfection for signs of illness, including weight loss, ruffled fur, ataxia, and seizures. Moribund mice were euthanized in accordance with IACUC guidelines. RNA was isolated from individual mice at the desired times postinfection using TriReagent (Sigma) and subjected to analysis as described above.

Immunofluorescence. Primary neurons and MEFs were plated on coverslips and treated as previously described. Coverslips were fixed using

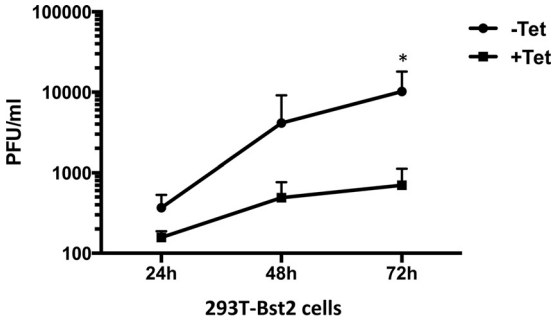

FIG 2 Bst2 expression reduces MV egress in nonneuronal cells. Supernatants were taken from MV-infected 293T-Bst2 cells with or without tetracycline at 24, 48, and 72 h postinfection. Results of at least 3 independent experiments are presented. Error bars are used to indicate the standard deviations among groups. The number of infectious virus particles released was determined by plaque assay. Data are considered significant as determined by ANOVA. *, $P < 0.05$. $n = 3$.

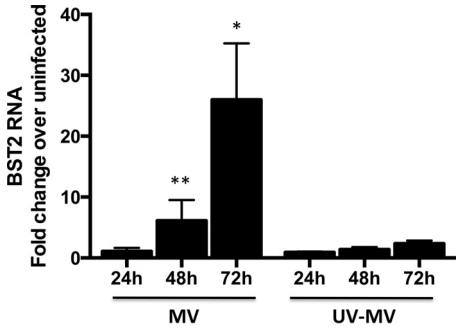

FIG 3 Viral infection induces Bst2 RNA synthesis in neurons. (A) Primary neurons infected with MV (MOI = 1) or challenged with the same dose of UV-inactivated MV were assayed for Bst2 RNA levels by RT-qPCR. Data are represented as fold change over the value for untreated cells using the $\Delta\Delta CT$ method. $n = 3$ per group. Results of at least 3 independent experiments are presented. Error bars are used to indicate the standard deviations among groups. Results for unpaired t test with equal-standard-deviation samples compared to the value for the uninfected control are shown. **, $P < 0.005$; *, $P < 0.05$.

4% paraformaldehyde–4% sucrose in phosphate-buffered saline (PBS), followed by further fixation and permeabilization with 100% methanol and then with 0.2% Triton in PBS. Coverslips were blocked with 10% goat serum and 10% fetal bovine serum in PBS. Primary antibodies for Bst2 (Sigma; 1:200) and mouse β-actin (Sigma; 1:2,000) were applied. Directly conjugated secondary antibodies were used (Hoechst, 1:1,000; donkey anti-rabbit AF488, 1:5,000; and goat anti-mouse AF555, 1:5,000). Coverslips were mounted to slides using Citifluor AF1 (Electron Microscopy Sciences) and sealed. Images were captured at 40× using an inverted TE2000 Nikon C1 confocal microscope.

Statistical analysis. Data representation and statistical analysis were performed using Prism GraphPad. Unpaired t test with equal standard deviations or analysis of variance (ANOVA) are shown. Figures represent the results of at least 3 independent experiments, unless otherwise noted in the figure legends. Samples were compared to an uninfected or untreated control. Significant differences are indicated by asterisks as follows: **, $P < 0.005$, and *, $P < 0.05$. Error bars are used to indicate the standard deviations.

RESULTS

Bst2 is induced following interferon exposure in neurons and MEFs. In a previous study, we identified the gene for bone marrow stromal antigen 2 (Bst2) as among the most highly induced neuronal genes following MV infection (23). To quantify this induction more fully, we cultured primary hippocampal neurons and fibroblasts from day 15 embryonic mice, as previously described (26, 28). Five days postplating, primary neurons and fibroblasts were exposed to 100 U/ml of murine recombinant type I IFN (IFN-β) or type II IFN (IFN-γ). As expected, IFN-treated neurons and MEFs showed a significant and rapid synthesis of Bst2 RNA relative to untreated cells (Fig. 1A and B). Treatment of both neurons and MEFs with IFN-β resulted in significantly greater induction of Bst2 RNA than treatment with IFN-γ. Interestingly, increases in Bst2 induction were up to 50-fold greater in neurons than in MEFs.

To confirm that the changes in gene expression correlated with protein accumulation, we examined Bst2 protein expression after IFN treatment by Western blotting and immunofluorescence. Little basal Bst2 was detected in neurons in the absence of IFN, but the amount increased appreciably following IFN exposure. No increase in protein accumulation was observed in MEFs (Fig. 1C). When examining Bst2 protein expression at the single cell level using immunofluorescence, similar results were observed: there was an appreciable increase in Bst2 protein expression in neurons but not MEFs (Fig. 1D). These data indicate that Bst2 gene induction and protein accumulation occur in both neurons and MEFs but that the magnitude of induction is greater in neurons.

Bst2 blocks MV egress in nonneuronal cells. The observation that Bst2 is induced in response to IFN exposure led us to assess the role of Bst2 in limiting MV release. We infected 293T Rex cells that had been engineered to contain a tetracycline-inducible Bst2 gene (here called 293T-Bst2 cells). Bst2 is not expressed in these cells in the absence of tetracycline (12). 293T-Bst2 cells expressing or not expressing Bst2 were infected with MV, and supernatants were collected at various times postinfection and titers determined (Fig. 2). As expected from studies of other enveloped viruses in dividing cells, Bst2 expression resulted in a >50-fold decrease in infectious MV released into the supernatant. This confirms that MV, like Ebola virus, HIV-1, and VSV, is susceptible to Bst2-mediated restriction.

Bst2 expression is significantly induced after viral infection in primary neurons. The observation that Bst2 can limit MV release, coupled with the knowledge that Bst2 is induced more abundantly in neuronal cell populations than dividing MEFs, led us to further explore the contribution of Bst2 in preventing MV spread and pathogenesis in neuronal cells. For these experiments, we used a transgenic mouse model in which CD46, one of three identified MV receptors, and the primary receptor for vaccine strains such as MV-Edmonston, is constitutively expressed under the transcriptional control of the neuron specific enolase promoter (NSE-CD46$^+$ mice), allowing for exclusively neuronal infection (24–26). Primary hippocampal neurons explanted from NSE-CD46$^+$ mice were challenged with MV-Edmonston. Expression of Bst2 RNA was significantly elevated in MV-infected neurons, increasing as the virus spread throughout the culture (Fig. 3). Induction was dependent on replicating virus, as UV-inactivated MV did not appreciably alter Bst2 expression levels. To confirm that Bst2's induction in response to viral infection was not unique to MV, we infected primary neurons with lymphocytic choriomeningitis virus (LCMV), another neurotropic, enveloped RNA virus. Again, a significant increase in Bst2 RNA expression

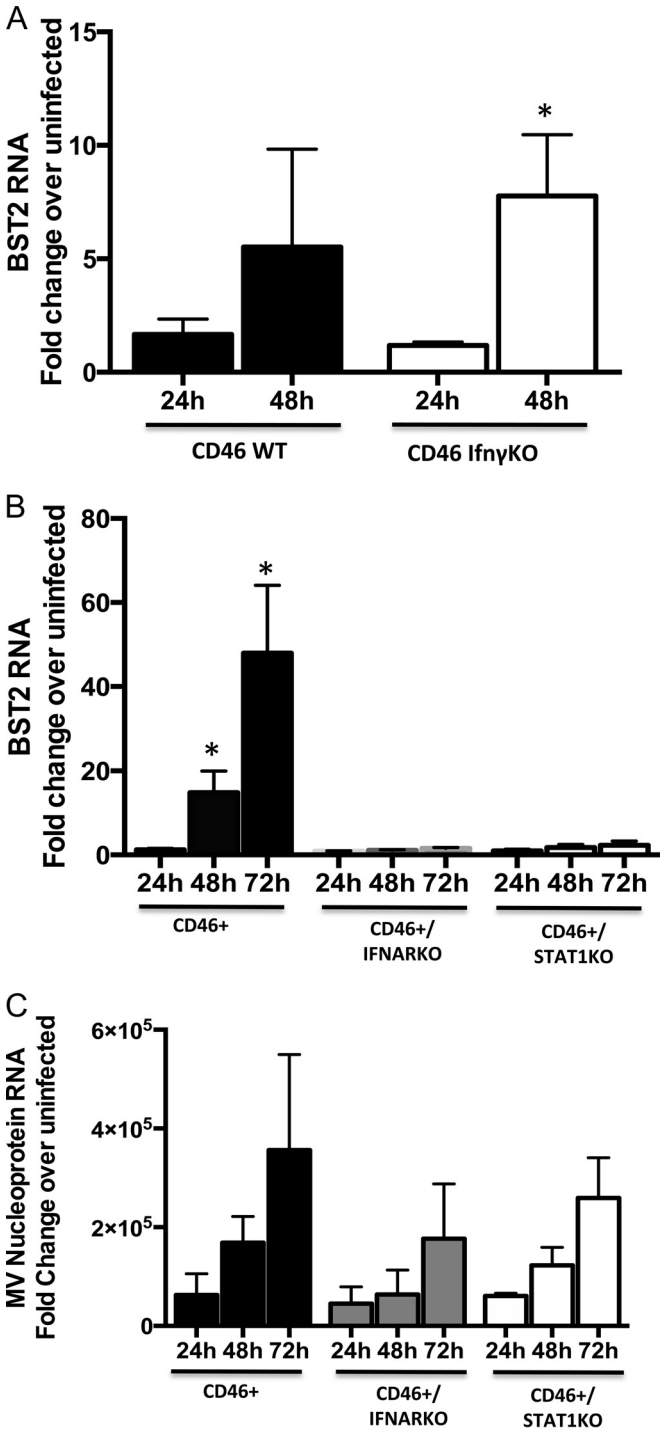

FIG 4 Bst2 induction in neurons is dependent on type I IFN signaling. (A) Primary CD46$^+$ and CD46$^+$/IFN-γ KO neurons were infected with MV for the indicated times and assayed for Bst2 RNA expression by RT-qPCR. (B) Primary NSE-CD46$^+$, NSE-CD46$^+$/Stat1 KO, and NSE-CD46$^+$/IFNAR KO neurons were infected with MV for the indicated period and assayed for Bst2 RNA expression. (C) Relative levels of MV nucleoprotein RNA in indicated genotypes of primary neurons. Data are presented as fold change over the value for uninfected neurons using the ΔΔ*CT* method. Results of at least 3 independent experiments are presented. Error bars represent the standard deviations among groups. $n = 3$ or 4 per group. Results for unpaired *t* test with equal-standard-deviation samples compared to the value for the uninfected control are shown. *, $P < 0.05$.

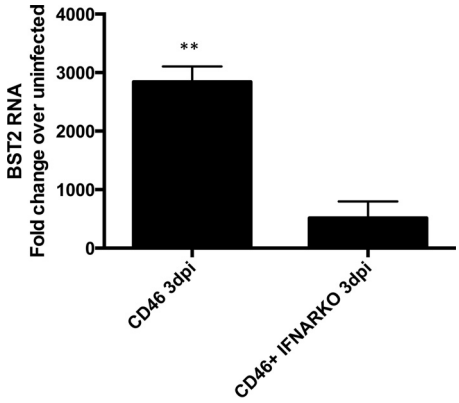

FIG 5 Bst2 expression is induced *in vivo* after MV infection via type I Ifn signaling. Mice of the indicated genotypes were infected intracranially with 1×10^4 PFU of the MV-Edmonston. Bst2 RNA expression in whole brains was assessed 3 dpi. Data are presented as fold change over the value for uninfected mice using the ΔΔ*CT* method. $n = 3$ or 4 per group. Error bars represent the standard deviations among groups. Results for npaired *t* test with equal-standard-deviation samples compared to the value for the uninfected control are shown. **, $P < 0.005$.

was observed, correlating with time postinfection (data not shown).

Bst2 induction in neurons is dependent on type I interferon signaling. To define how Bst2 is induced following MV infection, we utilized primary hippocampal neurons obtained from several knockout mice lacking key elements of the IFN response pathway. When CD46$^+$/IFN-γ knockout primary neurons were challenged with MV, Bst2 RNA was present at levels similar to those in control neurons at 24 and 48 h postinfection (Fig. 4A). Because neurons can produce type I IFN, we next infected CD46$^+$/IFNAR KO neurons (33), reasoning that though these neurons could synthesize type I IFNs in response to infection, the lack of a functional receptor would preclude them from mounting a transcriptional response to secreted IFNs. Indeed, the absence of a functional type I IFN receptor ablated the virus-induced synthesis of Bst2 at both 24 and 48 h postinfection (Fig. 4B). Even at 72 h postinfection, when MV had spread extensively through the culture, as assessed by increased levels of MV nucleoprotein RNA (Fig. 4C), Bst2 RNA levels remained unchanged. This finding was further supported when primary neurons isolated from mice lacking Stat1, a central signaling molecule in the type I IFN cascade, were also unable to induce Bst2 during virus infection (Fig. 4B). From these data, we conclude that primary neurons infected with MV synthesize Bst2 RNA through a Stat1-mediated signaling pathway that is triggered by type I IFN.

Bst2 expression is induced *in vivo* after MV infection via type I IFN signaling. To assess the role of type I IFN signaling in inducing Bst2 expression *in vivo*, we infected NSE-CD46$^+$ and NSE-CD46$^+$/IFNAR KO mice intracranially with 1×10^4 PFU of MV-Edmonston. All mice were monitored daily for signs of disease. At 3 days postinfection (dpi), animals were sacrificed and whole brains were examined for Bst2 induction via RT-qPCR. Mice that lacked the type I IFN receptor, and thus IFN signaling, were unable to induce Bst2 expression, in contrast to those with an intact IFN signaling pathway (Fig. 5). These *in vivo* data support the results obtained from our primary neuronal cultures and confirm type I IFN as a critical inducer of Bst2 synthesis in neurons after viral challenge.

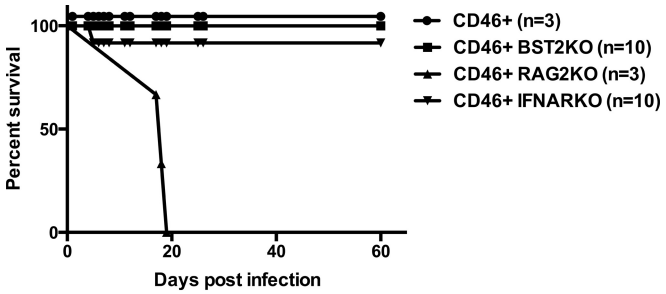

FIG 6 Bst2 is dispensable *in vivo* for survival after neuronal MV challenge. Mice of the indicated genotypes were infected intracranially with 1×10^4 PFU of MV-Edmonston.

Bst2 is dispensable *in vivo* for survival after neuronal MV challenge. We hypothesized that the strong induction of Bst2 in neurons after IFN exposure or viral challenge, as well as the reduction in MV release from Bst2 expressing 293T-Bst2 cells, might imply a critical role for this molecule in maintaining neuronal health by either contributing to an antiviral state or skewing the virus toward a mechanism of interneuronal spread. This was assessed following infection of various knockout mice. Bst2 KO mice and IFNAR KO mice were backcrossed to NSE-CD46$^+$ mice; all F_2 and F_3 progeny were screened for CD46 and Bst2 or IFNAR expression to ensure genotypes (data not shown). Adults were then challenged with MV. Surprisingly, the absence of Bst2 did not appreciably affect pathogenesis *in vivo*, while the absence of the type I IFN receptor (IFNAR), as well as its downstream signaling molecule Stat1, resulted in early mortality after infection for approximately 10 to 30% of infected mice (Fig. 6 and data not shown) (23, 34). All CD46/Bst2 KO mice survived infection, whereas control NSE-CD46$^+$/Rag2 KO mice, deficient in mature B and T cells, died as a consequence of unrestricted viral spread, as previously reported (Fig. 6) (30, 35). Moreover, both NSE-CD46$^+$ and NSE-CD46$^+$/Bst2 KO mice maintained their weight throughout the experiment, whereas NSE-CD46$^+$/Rag2 KO mice progressively wasted until they were euthanized (data not shown). Taken together, these data show that Bst2 is significantly induced in neurons and highly dependent on type I IFN signaling but is ultimately dispensable for survival after neuronal viral challenge *in vivo*.

DISCUSSION

Our findings underscore the importance of considering cell type specificity when evaluating antiviral responses. While both primary neurons and fibroblasts significantly upregulate Bst2 RNA and protein in response to viral infection and IFN exposure, primary mouse hippocampal neurons do so to a much greater extent. Although these neurons have low basal expression of many ISGs, their induction is appreciable after viral infection. The role or evolutionary advantage of lower homeostatic expression of key signaling molecules in neurons remains to be clearly defined (31, 36). While the well-studied ISG product Bst2 was significantly induced in primary neurons and *in vivo*, this protein appears to be dispensable for survival after neurotropic infection. Induced Bst2 expression was capable of suppressing MV release in 293T-Bst2 cells, making the lack of an effect of Bst2 following CNS viral challenge that much more surprising.

Previous studies from our laboratory, using mice deficient in the type I IFN receptor, IFNAR, or its downstream signaling molecule Stat1, showed that functional type I IFN signaling is important for the ability to survive a neuronal MV challenge *in vivo*, with >25% of mice succumbing to infection, and all surviving animals showing lasting signs of infection and neuropathology (23, 34). While the Edmonston strain of MV fully activates type I IFN signaling during infection, as opposed to wild-type (WT) strains, it is clear that the loss of type I IFN signaling results in CNS pathogenesis. The confirmation of Bst2 as one of the most highly induced ISG products in neurons led us to hypothesize that this gene may be a key effector in preventing MV-induced death and CNS disease, though our subsequent experiments indicated that this is not the case. It has been previously shown that the loss of Bst2 may hinder the ability of certain viruses to gain entry to a host cell, specifically influenza virus, vesicular stomatitis virus, and human cytomegalovirus (37, 38). Bst2 can modulate the actin network through a Rich2 complex, maintaining microvillus integrity (39). As MV spreads transsynaptically in CNS neurons, this function of Bst2 might help explain why Bst2 KO mice show no pathogenic consequences after MV infection, and it may imply an actin-mediated mechanism of neuronal MV transmission.

It is increasingly clear that neuronal viral infections are resolved by the host immune response differently from infections of renewable cells. Although perforin-mediated cell killing is a primary strategy to eliminate virus from rapidly dividing and renewable cell types, neurons are generally nonrenewable, and thus it has been proposed that these cytolytic strategies may be more harmful than beneficial within the brain. For a number of viral model systems, it has been shown that cytokine-mediated, noncytolytic strategies control many neurotropic infections (40–47). These data suggest that the mechanisms by which viral infections are resolved are exquisitely cell type specific and may reflect evolutionary pressures to restrict an infection while minimizing cytopathology and tissue damage. Even more, differences among neuronal subpopulations may further stratify the response to a viral infection, as was recently shown for West Nile virus (22). Our studies underscore the need to consider cell type differences when defining antiviral mechanisms; doing so may lead to more precisely tailored therapeutic strategies to resolve life-threatening viral encephalitic diseases.

ACKNOWLEDGMENTS

We thank Siddharth Balachandran, Christine M. Matullo, Kevin J. O'Regan, and Andreas C. Solomos for their contributions to this study and to the manuscript.

This work was supported by the following sources: grant R01 NS40500 (G.F.R.), grant F31 NS076202-01A1 (S.E.C.), grant T32 NS007180-32 (K.D.M.), a gift from the F. M. Kirby Foundation (G.F.R.), and grant P30CA006927 from the National Cancer Institute. The project described was supported by grant F31NS076202 from the National Institute of Neurological Disorders And Stroke.

The content of this article is solely the responsibility of the authors and does not necessarily represent the official views of the National Institute of Neurological Disorders and Stroke or the National Institutes of Health.

A.M.H., K.D.M., S.E.C., and G.F.R. conceived and designed the experiments; A.M.H. and K.D.M. performed the experiments; A.M.H., K.D.M, and G.F.R. analyzed the data; and A.M.H., K.D.M., and G.F.R. wrote the paper.

REFERENCES

1. **Goodbourn S, Didcock L, Randall RE.** 2000. Interferons: cell signalling, immune modulation, antiviral responses and virus countermea-

sures. J Gen Virol **81:**2341–2364. http://dx.doi.org/10.1099/0022-1317-81-10-2341.
2. **Sorgeloos F, Kreit M, Hermant P, Lardinois C, Michiels T.** 2013. Antiviral type I and type III interferon responses in the central nervous system. Viruses **5:**834–857. http://dx.doi.org/10.3390/v5030834.
3. **Snell LM, Brooks DG.** 2015. New insights into type I interferon and the immunopathogenesis of persistent viral infections. Curr Opin Immunol **34:**91–98. http://dx.doi.org/10.1016/j.coi.2015.03.002.
4. **Blasius AL, Giurisato E, Cella M, Schreiber RD, Shaw AS, Colonna M.** 2006. Bone marrow stromal cell antigen 2 is a specific marker of type I IFN-producing cells in the naive mouse, but a promiscuous cell surface antigen following IFN stimulation. J Immunol **177:**3260–3265. http://dx.doi.org/10.4049/jimmunol.177.5.3260.
5. **Goto T, Kennel SJ, Abe M, Takishita M, Kosaka M, Solomon A, Saito S.** 1994. A novel membrane antigen selectively expressed on terminally differentiated human B cells. Blood **84:**1922–1930.
6. **Neil SJD, Zang T, Bieniasz PD.** 2008. Tetherin inhibits retrovirus release and is antagonized by HIV-1 Vpu. Nature **451:**425–430. http://dx.doi.org/10.1038/nature06553.
7. **Fitzpatrick K, Skasko M, Deerinck TJ, Crum J, Ellisman MH, Guatelli J.** 2010. Direct restriction of virus release and incorporation of the interferon-induced protein BST-2 into HIV-1 particles. PLoS Pathog **6**(3): e1000701. http://dx.doi.org/10.1371/journal.ppat.1000701.
8. **Perez-Caballero D, Zang T, Ebrahimi A, McNatt MW, Gregory DA, Johnson MC, Bieniasz PD.** 2009. Tetherin inhibits HIV-1 release by directly tethering virions to cells. Cell **139:**499–511. http://dx.doi.org/10.1016/j.cell.2009.08.039.
9. **Van Damme N, Goff D, Katsura C, Jorgenson RL, Mitchell R, Johnson MC, Stephens EB, Guatelli J.** 2008. The interferon-induced protein BST-2 restricts HIV-1 release and is downregulated from the cell surface by the viral Vpu protein. Cell Host Microbe **3:**245–252. http://dx.doi.org/10.1016/j.chom.2008.03.001.
10. **Hammonds J, Wang J-J, Yi H, Spearman P.** 2010. Immunoelectron microscopic evidence for tetherin/BST2 as the physical bridge between HIV-1 virions and the plasma membrane. PLoS Pathog **6**(2):e1000749. http://dx.doi.org/10.1371/journal.ppat.1000749.
11. **Kaletsky RL, Francica JR, Agrawal-Gamse C, Bates P.** 2009. Tetherin-mediated restriction of filovirus budding is antagonized by the Ebola glycoprotein. Proc Natl Acad Sci U S A **106:**2886–2891. http://dx.doi.org/10.1073/pnas.0811014106.
12. **Weidner JM, Jiang D, Pan XB, Chang J, Block TM, Guo JT.** 2010. Interferon-induced cell membrane proteins, IFITM3 and tetherin, inhibit vesicular stomatitis virus infection via distinct mechanisms. J Virol **84:** 12646–12657. http://dx.doi.org/10.1128/JVI.01328-10.
13. **Liu Y, Luo S, He S, Zhang M, Wang P, Li C, Huang W, Hu B, Griffin GE, Shattock RJ.** 2015. Tetherin restricts HSV-2 release and is counteracted by multiple viral glycoproteins. Virology **475:**96–109. http://dx.doi.org/10.1016/j.virol.2014.11.005.
14. **Hotter D, Sauter D, Kirchhoff F.** 2013. Emerging role of the host restriction factor tetherin in viral immune sensing. J Mol Biol **425:**4956–4964. http://dx.doi.org/10.1016/j.jmb.2013.09.029.
15. **Martin-Serrano J, Neil SJD.** 2011. Host factors involved in retroviral budding and release. Nat Rev Microbiol **9:**519–531. http://dx.doi.org/10.1038/nrmicro2596.
16. **Evans DT, Serra-Moreno R, Singh RK, Guatelli JC.** 2010. BST-2/tetherin: a new component of the innate immune response to enveloped viruses. Trends Microbiol **18:**388–396. http://dx.doi.org/10.1016/j.tim.2010.06.010.
17. **Cocka LJ, Bates P.** 2012. Identification of alternatively translated tetherin isoforms with differing antiviral and signaling activities. PLoS Pathog **8**(9):e1002931. http://dx.doi.org/10.1371/journal.ppat.1002931.
18. **Jia X, Weber E, Tokarev A, Lewinski M, Rizk M, Suarez M, Guatelli J, Xiong Y.** 2014. Transmembrane helices are represented by cylinders and the Nef myristoyl anchor is represented by a cyan sphere. Elife **3:**1–24. http://dx.doi.org/10.7554/eLife.02362.
19. **Serra-Moreno R, Zimmermann K, Stern LJ, Evans DT.** 2013. Tetherin/BST-2 antagonism by Nef depends on a direct physical interaction between Nef and tetherin, and on clathrin-mediated endocytosis. PLoS Pathog **9**(7):e1003487. http://dx.doi.org/10.1371/journal.ppat.1003487.
20. **Masuyama N, Kuronita T, Tanaka R, et al.** 2009. HM1.24 is internalized from lipid rafts by clathrin-mediated endocytosis through interaction with adaptin. J Biol Chem **284:**15927–15941. http://dx.doi.org/10.1074/jbc.M109.005124.
21. **Sarojini S, Theofanis T, Reiss CS.** 2011. Interferon-induced tetherin restricts vesicular stomatitis virus release in neurons. DNA Cell Biol **30:** 965–974. http://dx.doi.org/10.1089/dna.2011.1384.
22. **Cho H, Proll SC, Szretter KJ, Katze MG, Gale M, Diamond MS.** 2013. Differential innate immune response programs in neuronal subtypes determine susceptibility to infection in the brain by positive-stranded RNA viruses. Nat Med **19:**458–464. http://dx.doi.org/10.1038/nm.3108.
23. **O'Donnell LA, Conway S, Rose RW, Nicolas E, Slifker M, Balachandran S, Rall GF.** 2012. STAT1-independent control of a neurotropic measles virus challenge in primary neurons and infected mice. J Immunol **188:** 1915–1923. http://dx.doi.org/10.4049/jimmunol.1101356.
24. **Naniche D, Varior-Krishnan G, Cervoni F, Wild TF, Rossi B, Rabourdin-Combe C, Gerlier D.** 1993. Human membrane cofactor protein (CD46) acts as a cellular receptor for measles virus. J Virol **67:**6025–6032.
25. **Dörig RE, Marcil A, Chopra A, Richardson CD.** 1993. The human CD46 molecule is a receptor for measles virus (Edmonston strain). Cell **75:**295–305. http://dx.doi.org/10.1016/0092-8674(93)80071-L.
26. **Rall GF, Manchester M, Daniels LR, Callahan EM, Belman AR, Oldstone MBA.** 1997. A transgenic mouse model for measles virus infection of the brain. Proc Natl Acad Sci U S A **94:**4659–4663. http://dx.doi.org/10.1073/pnas.94.9.4659.
27. **Makhortova NR, Askovich P, Patterson CE, Gechman LA, Gerard NP, Rall GF.** 2007. Neurokinin-1 enables measles virus trans-synaptic spread in neurons. Virology **362:**235–244. http://dx.doi.org/10.1016/j.virol.2007.02.033.
28. **Lawrence DMP, Patterson CE, Gales TL, D'Orazio JL, Vaughn MM, Rall GF.** 2000. Measles virus spread between neurons requires cell contact but not CD46 expression, syncytium formation, or extracellular virus production. J Virol **74:**1908–1918. http://dx.doi.org/10.1128/JVI.74.4.1908-1918.2000.
29. **Lawrence DMP, Vaughn MM, Belman AR, Cole JS, Rall GF.** 1999. Immune response-mediated protection of adult but not neonatal mice from neuron-restricted measles virus infection and central nervous system disease. J Virol **73:**1795–1801.
30. **Patterson CE, Lawrence DMP, Echols LA, Rall GF.** 2002. Immune-mediated protection from measles virus-induced central nervous system disease is noncytolytic and gamma interferon dependent. J Virol **76:**4497–4506. http://dx.doi.org/10.1128/JVI.76.9.4497-4506.2002.
31. **Rose RW, Vorobyeva AG, Skipworth JD, Nicolas E, Rall GF.** 2007. Altered levels of STAT1 and STAT3 influence the neuronal response to interferon gamma. J Neuroimmunol **192:**145–156. http://dx.doi.org/10.1016/j.jneuroim.2007.10.007.
32. **National Research Council.** 2011. Guide for the care and use of laboratory animals, 8th ed. National Academies Press, Washington, DC.
33. **Delhaye S, Paul S, Blackqori G, Minet M, Weber F, Staeheli P, Michiels T.** 2006. Neurons produce type I interferon during viral encephalitis. Proc Natl Acad Sci U S A **103:**7835–7840. http://dx.doi.org/10.1073/pnas.0602460103.
34. **Cavanaugh SE, Holmgren AM, Rall GF.** 2015. Homeostatic interferon expression in neurons is sufficient for early control of viral infection. J Neuroimmunol **279:**11–19. http://dx.doi.org/10.1016/j.jneuroim.2014.12.012.
35. **Tishon A, Lewicki H, Andaya A, McGavern D, Martin L, Oldstone MBA.** 2006. CD4 T cell control primary measles virus infection of the CNS: regulation is dependent on combined activity with either CD8 T cells or with B cells: CD4, CD8 or B cells alone are ineffective. Virology **347:** 234–245. http://dx.doi.org/10.1016/j.virol.2006.01.050.
36. **Podolsky MA, Solomos AC, Durso LC, Evans SM, Rall GF, Rose RW.** 2012. Extended JAK activation and delayed STAT1 dephosphorylation contribute to the distinct signaling profile of CNS neurons exposed to interferon-gamma. J Neuroimmunol **251:**33–38. http://dx.doi.org/10.1016/j.jneuroim.2012.06.006.
37. **Viswanathan K, Smith MS, Malouli D, Mansouri M, Nelson JA, Früh K.** 2011. BST2/tetherin enhances entry of human cytomegalovirus. PLoS Pathog **7**(11):e1002332. http://dx.doi.org/10.1371/journal.ppat.1002332.
38. **Swiecki M, Wang Y, Gilfillan S, Lenschow DJ, Colonna M.** 2012. Cutting edge: paradoxical roles of BST2/tetherin in promoting type I IFN response and viral infection. J Immunol **188:**2488–2492. http://dx.doi.org/10.4049/jimmunol.1103145.
39. **Rollason R, Korolchuk V, Hamilton C, Jepson M, Banting G.** 2009. A CD317/tetherin-RICH2 complex plays a critical role in the organization of the subapical actin cytoskeleton in polarized epithelial cells. J Cell Biol **184:**721–736. http://dx.doi.org/10.1083/jcb.200804154.

40. **Burdeinick-Kerr R, Govindarajan D, Griffin DE.** 2009. Noncytolytic clearance of Sindbis virus infection from neurons by gamma interferon is dependent on Jak/Stat signaling. J Virol **83:**3429–3435. http://dx.doi.org/10.1128/JVI.02381-08.
41. **Griffin DE.** 2010. Recovery from viral encephalomyelitis: immune-mediated noncytolytic virus clearance from neurons. Immunol Res **47:**123–133. http://dx.doi.org/10.1007/s12026-009-8143-4.
42. **Patterson CE, Daley JK, Rall GF.** 2002. Neuronal survival strategies in the face of RNA viral infection. J Infect Dis **186:**215–219.
43. **Griffin DE, Metcalf T.** 2011. Clearance of virus infection from the CNS. Curr Opin Virol **1:**216–221. http://dx.doi.org/10.1016/j.coviro.2011.05.021.
44. **St Leger AJ, Hendricks RL.** 2011. CD8+ T cells patrol HSV-1-infected trigeminal ganglia and prevent viral reactivation. J Neurovirol **17:**528–534. http://dx.doi.org/10.1007/s13365-011-0062-1.
45. **Liu T, Khanna KM, Chen X, Fink DJ, Hendricks RL.** 2000. CD8+ T cells can block herpes simplex virus type 1 (HSV-1) reactivation from latency in sensory neurons. J Exp Med **191:**1459–1466. http://dx.doi.org/10.1084/jem.191.9.1459.
46. **Wakim LM, Woodward-Davis A, Liu R, et al.** 2012. The molecular signature of tissue resident memory CD8 T cells isolated from the brain. J Immunol **189:**3462–3471. http://dx.doi.org/10.4049/jimmunol.1201305.
47. **Wakim LM, Woodward-Davis A, Bevan MJ.** 2010. Memory T cells persisting within the brain after local infection show functional adaptations to their tissue of residence. Proc Natl Acad Sci U S A **107:**17872–17879. http://dx.doi.org/10.1073/pnas.1010201107.